Design of Anti-Windup-Extensions for digital control loops

St. Lambeck and O. Sawodny
Institute of Automation and System Science
Technische Universität Ilmenau
PO. Box 100565, 98684 Ilmenau, Germany

Abstract— **In this paper, two design methods for "Anti-Windup"(AW)-Extensions based on bode plots will be proposed. Most control engineers are familiar with the frequency response characteristics. Therefore the methods can easily be applied. For applications with a large operating area, a new adaptive structure of the AW-Extension is suggested. The influence of measurement noise on control loops with a constrained control signal will also be investigated using frequency response characteristics.**

I. INTRODUCTION

Nonlinearities, caused by constraints in the actuators are often found in control loops and lead to a remarkable deterioration of the control performance - the so-called "Windup"-effect. In history, a lot of schemes for control design to deal with this effect have been developed, which are often based on heuristic rules or are limited to a specific class of controllers (for instance PI-/PID-Controllers). General approaches are proposed in [1], [2]. All these schemes are termed as "Anti-Windup"(AW)-schemes.

In this work, the design of an extension for the linear designed controller (AW-Extension), based on the idea in [5] and [6], is proposed. The design procedure is based on a simple scheme, which uses the bode plot of the linear part of a nonlinear standard control loop. This can then be easily applied to digital control loops after a bilinear transformation. The stability properties of the closed loop system with the extended controller can be affected by the choice of the AW-Extension. Another advantage of the proposed scheme is the possibility of conversion from the extended controller in other popular AW-schemes, like the "Conditioning technique" (CT) [8] or the "Observer based Anti-Windup" [1], and vice versa. Stability and performance properties of these schemes can be analyzed and compared in that way.

In order to cover a large operating range, the AW-Extension includes an adaptive tuning parameter. This new structure leads to a better performance in case of large setpoint changes in control applications compared to an AW-Extension with fixed parameters.

The influence of measurement noise on control performance of the control loop with an extended AW-Controller is usually neglected and not further investigated by most authors. It will be shown in this paper that measurement noise can have a significant influence on the control behaviour under certain conditions.

The design of the AW-Extension will be explained in II. The above mentioned adaptive approach will be presented in III. A discussion about the influence of measurement noise follows in IV.

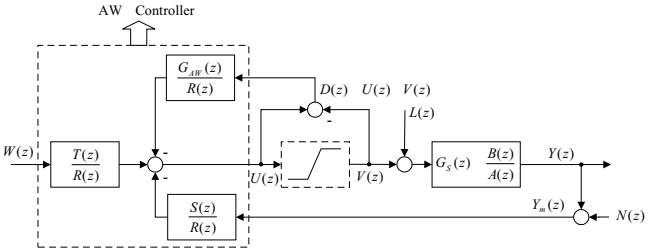

Fig. 1. Controller with AW-Extension

II. DESIGN OF THE AW-EXTENSION

A. The extended compensator structure

Based on the work of Chan and Hui [6], [5] the difference between the unconstrained and constrained control signals will be interpreted as a nonlinear "disturbance" D. In order to reduce the effects of saturation, a structure similar to a feedforward control is proposed. Fig. 1 shows the structure of the control loop where W, L and N denote the setpoint, a load disturbance and measurement noise respectively. According to Fig. 1 the system output results in (the Argument z will be neglected):

$$Y = \underbrace{\frac{B}{A\cdot R + B\cdot S}\cdot(T\cdot W - R\cdot L - S\cdot N)}_{Y_{lin}} - \underbrace{\frac{(G_{AW}+R)\cdot B}{A\cdot R + B\cdot S}}_{H_D}\cdot D \tag{1}$$

The design task is to find a suitable transfer function G_{AW}, which reduces the "disturbance"-effects to an acceptable minimum. The term H_D in (1) represents the transfer function from the fictitious "disturbance" D to the system output Y and can be varied by the choice of the poles and zeros of G_{AW}. At first sight, one should attempt to make H_D in (1) sufficiently fast in order to avoid the influence of D proceeding for a long time after desaturation. But it must not be made too fast because of possible saturation of the control signal in the opposite direction. So the design of G_{AW} becomes a pole-zero-placement problem. Unfortunately, a suitable pole and zero allocation depends on the definite bounds of the control signal and stability problems can occur under specific conditions (see also [2]). In the following a second, more systematic way of finding G_{AW} will be described in more details. It is based on the describing function method for stability analysis.

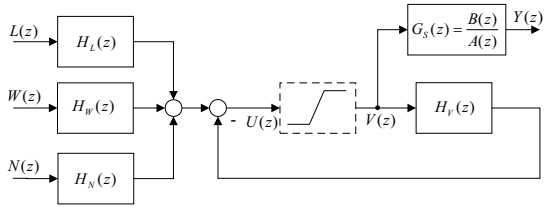

Fig. 2. Resulting nonlinear standard control loop

B. Use of frequency response characteristics

The structure in Fig. 1 can be easily transformed into a nonlinear standard control loop as shown in Fig. 2. The unconstrained control signal can be expressed as follows:

$$U = \underbrace{\frac{1}{R+G_{AW}} \cdot (T \cdot W - S \cdot G_s \cdot L - S \cdot N)}_{H_W, H_L, H_N} - \underbrace{\frac{G_s \cdot S - G_{AW}}{R+G_{AW}}}_{H_V} \cdot V \tag{2}$$

Different methods of stability analysis for nonlinear systems in the frequency domain, such as the Popov-criterion and the Circle criterion, can be applied to the structure in Fig. 2. An easy to use method for the prediction of limit cycle oscillations is the describing function analysis, where intersections between the Nyquist curve of the linear part H_V and the negative inverse describing function of the saturation element indicates the appearance of limit cycle oscillations. To make the method applicable to digital control systems, it is recommended to use the following bilinear transformation of the complex variable z:

$$z = e^{s \cdot T_a} = \frac{1 + \frac{T_a}{2} w}{1 - \frac{T_a}{2} w} \qquad \Leftrightarrow \qquad w = \frac{2}{T_a} \cdot \frac{z-1}{z+1} \tag{3}$$

The complex variable w is defined as:

$$w = \xi + j\Omega \tag{4}$$

Thus, a transformed frequency Ω in the range from 0 to ∞ is dedicated to the real frequency ω in the range from 0 to $\frac{\pi}{T_a}$.
The negative inverse describing function of the saturation lies on the negative real axis in the $j\Omega$-plane in the range from -1 to $-\infty$. From this it follows that for the limit cycle prediction it is sufficient to investigate the phase response of $H_V(j\Omega)+1$ subject to -180°. With

$$\alpha = A \cdot R + B \cdot S \tag{5}$$

as the characteristic polynomial of the closed loop, the following relation results from (2):

$$H_V + 1 = \frac{\alpha}{A \cdot (R + G_{AW})} \tag{6}$$

Based on the idea in [6], a possible approach for the design of G_{AW} is the use of a first-order transfer function F:

$$G_{AW} = \frac{T}{t_0 \cdot F} - R \quad \Rightarrow \quad H_V + 1 = \underbrace{\frac{\alpha \cdot t_0}{A \cdot T}}_{H_h} \cdot F \tag{7}$$

This approach implies two advantages. First, a good comparability to the above mentioned CT is guaranteed, because $F = 1$ [6], [9]. Another advantage is anchored in the special shape of the term $H_V + 1$ in (7). As easily can be seen, a possibly needed phase shifting of $H_V + 1$ required to guarantee a sufficient distance of the phase response from -180° (which avoids the occurrence of limit cycles) can be achieved by a suitable choice of the transfer function F as a phase-lead filter in the following form:

$$F(j\Omega) = \frac{Z_F(j\Omega)}{N_F(j\Omega)} = \frac{\alpha_F \cdot \beta \cdot j\Omega + \alpha_F}{\alpha_F \cdot \beta \cdot j\Omega + 1} \tag{8}$$

The parameters α_F and β result from a known phase shifting ϕ_{max} at the frequency Ω_{max}:

$$\alpha_F = \frac{1 - \sin\phi_{max}}{1 + \sin\phi_{max}} \qquad \beta = \frac{1}{\Omega_{max} \cdot \sqrt{\alpha_F}} \tag{9}$$

The design can be summarized as follows:

- Use of the bilinear transformation (3) on $H_h(z)$ which leads to $H_h(j\Omega)$
- Plot of the phase response of $H_h(j\Omega)$ and check if $\phi_{min}\{H_h(j\Omega)\} < -135^\circ$
- if $\phi_{min}\{H_h(j\Omega)\} > -135^\circ \Rightarrow$ choose $F(j\Omega) = 1$ (no additional phase shift is required)
- if $\phi_{min}\{H_h(j\Omega)\} < -135^\circ \Rightarrow$ choose $F(j\Omega$ as a phase-lead filter (8), where the required phase-shift is

$$\phi_{max} = -135^\circ - \phi_{min}\{H_h(j\Omega)\} \tag{10}$$

- Transformation from $F(j\Omega)$ to $F(z)$ and determination of $G_{AW}(z)$ as in (7)

So the design of the AW-Extension reduces to the determination of a first order filter. The effectiveness of this method will be demonstrated on an example stated below.
The above described method works well if a clear minimum of the phase response exists. If this is not the case, a different approach using the magnitude of $H_V(j\Omega)+1$ can be applied. Therefore, the known design technique from linear theory of compliance with a defined phase reserve at the gain crossover frequency will be used for the nonlinear control loop. If we assume $F = 1$, then the transfer function from W to U following (2) becomes $H_W = t_0$. This means that after a setpoint change the maximal unconstrained control signal is made up of the step height w_0 and the leading coefficient of the T-Polynomial to $u_{max} = w_0 \cdot t_0$. If we define $k = \frac{y_{max}}{u_{max}}$ as the ratio of the maximal constrained and unconstrained control signal, then k represents the "degree of saturation" of the nonlinearity. The saturation element in Fig. 2 will now be replaced by k and the stability of the nonlinear standard control loop can be proved using the Aizerman conjecture. The characteristic equation of the standard control loop in Fig. 2 using k for the saturation element can also be used for the determination of F (and so G_{AW}) in (7):

$$1 + k \cdot (H_h \cdot F - 1) = 0 \quad \Rightarrow \quad k \cdot H_h \cdot F = -1 + k \tag{11}$$

The first order transfer function F can be determined so that at the gain crossover frequency $|k \cdot H_h(j\Omega)| = |-1+k|$ a predefined phase reserve (for instance 45°) is maintained. The design is as follows:

- Use of (3) on $k \cdot H_h(z) = \frac{k \cdot \alpha \cdot t_0}{A \cdot T}$ which leads to $H_h(j\Omega)$ which leads to $k \cdot H_h(j\Omega)$
- Definition of $\Omega_D = \Omega(|k \cdot H_h(j\Omega)|)_{dB} = |-1+k|_{dB}$ in the bode plot as the gain crossover frequency
- if $\phi(\Omega_D) > -135° \Rightarrow$ choose $F(j\Omega) = 1$ (no additional phase shift is required)
- if $\phi(\Omega_D) < -135° \Rightarrow$ choose $F(j\Omega)$ as a phase-lead filter (8), where the required phase-shift is determined as $\phi_{max} = -135° - \phi(\Omega_D)$ and $\Omega_{max} = \Omega_D$
- Transformation from $F(j\Omega)$ to $F(z)$ and determination of $G_{AW}(z)$ following (7)

The application of this second approach will be illustrated by another example in the following subsection.

C. Example

The following example was studied by Rönnbäck in [3] and here it will be shown that the first approach described above is often sufficient for a good control performance. The model is oscillative and represents the belt tension dynamics of a coupled electric drives laboratory process. The sampling time is set to $T_a = 20ms$ and the control signal is restricted to $v_{max} = -v_{min} = 10$.

$$G_S(z) = \frac{0.19z^{-3} + 0.01z^{-4} + 0.088z^{-5}}{1 - 2.98z^{-1} + 3.86z^{-2} - 2.5z^{-3} + 0.67z^{-4}} \quad (12)$$

The controller was designed by LQG-Optimization with following polynomials:

$$R(z) = 1 - 0.8z^{-1} + 0.63z^{-2} - 0.56z^{-3} - 0.07z^{-4} - 0.2z^{-5}$$

$$S(z) = 0.47 - 2.54z^{-1} + 5.2z^{-2} - 4.52z^{-3} + 1.43z^{-4} \quad (13)$$

$$T(z) = 2.19 - 5.25z^{-1} + 4.72z^{-2} - 1.89z^{-3} + 0.28z^{-4}$$

The phase responses are plotted in Fig. 3. The phase minimum of $H_h(j\Omega)$ lies at $-203°$. So a phase shifting of 68° with the use of $F(j\Omega)$ is necessary. The application of the first design approach described above (7-10) results in the desired transfer function of the AW-Extension. The system output after a setpoint change for two different operating points is shown in Fig. 4. To demonstrate the advantage of the proposed method, the curves, which result from the use of the CT ($F = 1$) are also plotted in the same figure. With the CT limit cycles arising in one operating point (which can be excepted by consideration of the phase response in Fig. 3), while the use of the proposed method leads to a smooth control performance.

The success of the second way of design will be demonstrated by another example. The plant can be described by a discrete I^2-Model and the controller is designed using the algebraic design method with the allegation of a desired

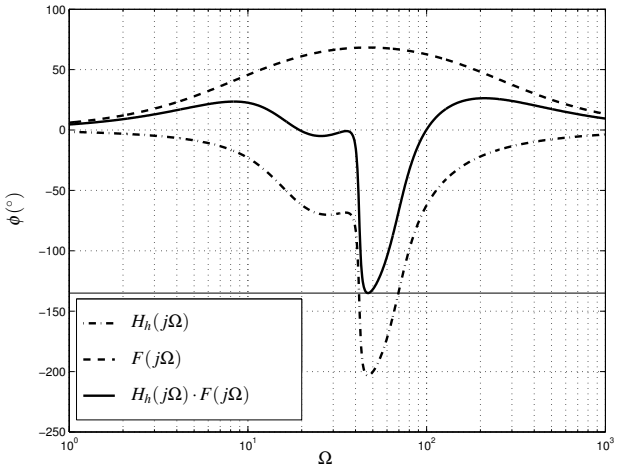

Fig. 3. Phase responses of simulation example 1

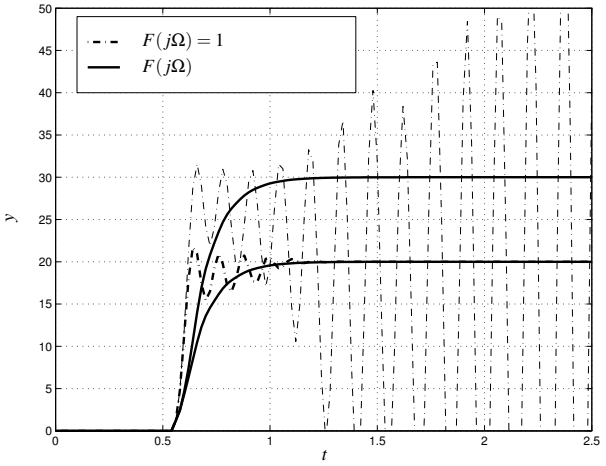

Fig. 4. System output of simulation example 1

closed loop transfer function and a sampling time of $T_a = 1s$:

$$G_S(z) = \frac{0.5 \cdot z + 0.5}{z^2 - 2 \cdot z + 1} \quad ; \quad G_W(z) = \frac{0.18 \cdot z + 0.18}{z^2 - 0.8 \cdot z + 0.16}$$

$$\begin{aligned} T(z) &= 0.36 \cdot z^2 - 0.576 \cdot z + 0.2304 \\ S(z) &= 0.7876 \cdot z^2 - 1.3904 \cdot z + 0.6172 \\ R(z) &= z^2 - 0.7983 \cdot z - 0.2062 \end{aligned} \quad (14)$$

The control signal is restricted to $|v|_{max} = 0.01$. A step in the setpoint with height $w_0 = 1$ results in $k = 0.0278$ and for $w_0 = 3$ we get $k = 0.0093$. The gain crossover frequency at $|k \cdot H_h(j\Omega)|_{dB} = |-1+k|_{dB}$ is not significantly different in these two cases. For a step with $w_0 = 1$ a gain crossover frequency $\Omega_D = 0.01014s^{-1}$ and a phase shift $\phi_{max} = 31.5°$ are resulting. The phase responses are shown in Fig. 5 and the system output for the two different setpoint changes is shown in Fig. 6 compared to the curves resulting from the use of the CT. It can be seen that the use of the CT results in a tendency to oscillations while the proposed method works well for the two operating points.

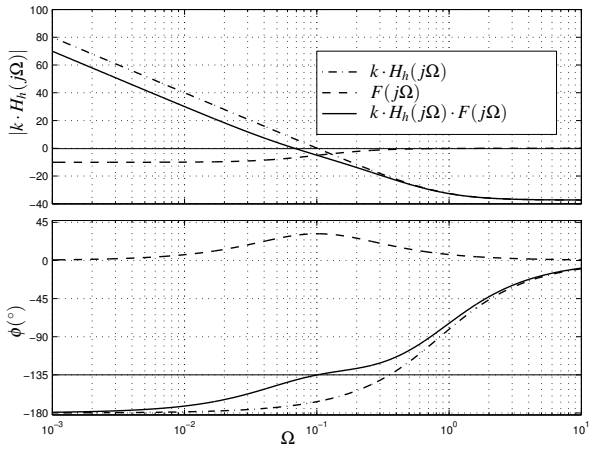

Fig. 5. Phase responses of simulation example 2

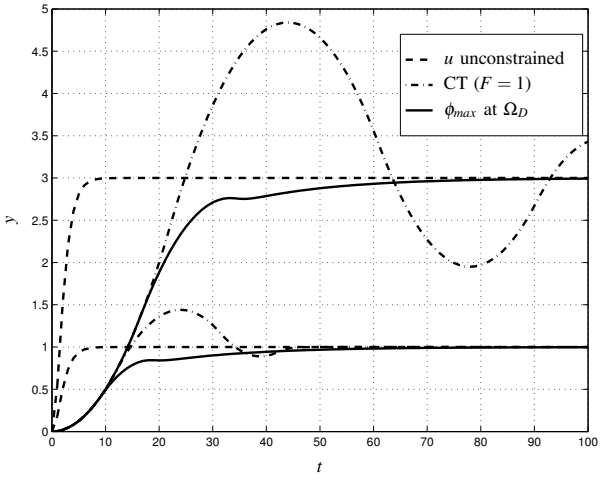

Fig. 6. System output of simulation example 2

III. Adaptive approach for the AW-Extension

In this section the influence of a free tuning parameter in the AW-Extension on the control performance will be investigated first. The use of this parameter is in particular advantageous for applications with a large operating area. Based on the results, an adaptive approach for the AW-Extension will be proposed.

A. AW-Extension with a free tuning parameter

The above mentioned interpretation of the saturation effect as a nonlinear "disturbance" D is the fundament of the following ideas. For a fast decay of this disturbance, sufficiently fast poles of H_D (see (1), which are influenced by the poles of the characteristic polynomial α and the poles of the AW-Extension G_{AW}, are necessary. If we choose F as a first order transfer function, the following approach with a free tuning parameter γ leads to satisfactory results:

$$F(z) = \frac{(z-\gamma)}{z} \quad \Rightarrow \quad F(j\Omega) = \frac{(1+\gamma)\cdot\{\frac{1-\gamma}{1+\gamma} + j\Omega\cdot\frac{T_a}{2}\}}{1+j\Omega\cdot\frac{T_a}{2}} \tag{15}$$

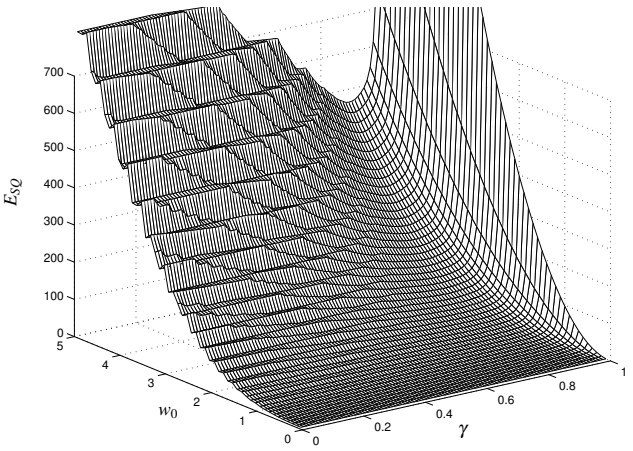

Fig. 7. Squared control error for the I^2-Plant

The amount of phase shifting rises with a growing γ in direction 1. Unfortunately, also a deceleration of the dynamics in H_D is the consequence. So the choice of a suitable γ is a compromise between the conflicting demands of a fast decay of the disturbance D and a larger stability margin served by a larger phase shifting. In Fig. 7 the dependency of the sum squared control error E_{SQ} from the height of the step in the setpoint and the parameter γ for the I^2-Plant is mapped. A larger w_0 requires a larger value of γ.

B. Development of the adaptive structure

The AW-Extension with the free tuning parameter γ will now be modified, so that γ is automatically adjusted with respect to the length and depth of the disturbance D. The proposed design of the AW-Extension is based on the idea presented by Rönnbäck in [4]. There, the linear designed controller is modified against the saturation effect. Here, the parameter γ of the AW-Extension will be varied subject to the "disturbance" D. We do not use the current value of D but a value, filtered by a first order transfer function. So we get information about the duration of the control signal in the saturation phase. Fig. 8 shows the structure of the control loop with the adaptive AW-Extension. The "Windupsignal" μ results in

$$\mu = \frac{z}{z - e^{-Ta\cdot\lambda\cdot\tau}} \cdot \left|\frac{D}{v_{max}}\right| \quad ; \quad \tau = e^{-\mu/K} \tag{16}$$

and comprised information about the saturation phase of the control signal, which can be used for the determination of γ. Roughly speaking, a large value of μ is the consequence of a distinct "disturbance" D. The parameters λ and K in (16) can be arbitrarily chosen. λ determines the time constant of the filter significantly and should be accurately determined, so that μ approaches 0 in an adequate time if the control signal is unconstrained for a while. An empirical formula for λ for the continuous case and the modification of the whole controller was developed in [4]. For our task the

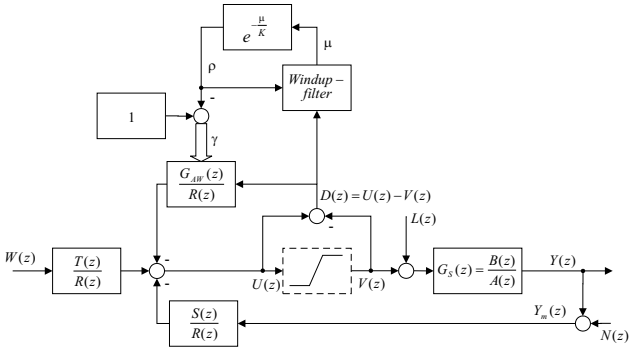

Fig. 8. Controller with adaptive AW-Extension

following term, that is suitable for digital applications, leads to satisfactory results in most cases:

$$\lambda = 0.1 \cdot \frac{\log(z_\alpha)}{T_a} \tag{17}$$

with z_α representing the location of the dominating poles in the z-Plane. The time constant of the filter is also determined by the so-called "fastness variable" τ. A small value of τ leads here to a large time constant. Also μ is a component of τ and a small value of τ implies a large value of μ (following (16)) and marks an undesirable disturbance D. In such cases a large value of the free parameter γ of the AW-Extension is advantageous because of the large stability margin required. So the following relation for γ seems to be most promising:

$$\gamma = 1 - \tau = 1 - e^{-\mu/K} \tag{18}$$

The parameter K can be used for fine-tuning. A larger value of K leads to a larger value of τ and so to a smaller value of γ. The function of the adaptive structure will now be demonstrated by a simulation of the above described control of the coupled electric drives ((12) and (13)). In Fig. 9 and Fig. 10 the system output and the curve of the free parameter γ for two different operating points are shown. The control performance is much better than with the use of a fixed parameter (see Fig. 4).

IV. Effect of measurement noise

The influence of measurement noise is treated only in a few publications [7], [10], because most authors assume consequences only in the linear range. But it can be shown that, induced by the stochastic character of the disturbance, under certain circumstances a significant influence of the measurement noise appears. This influence can also be investigated by the use of frequency response characteristics. Following Fig. 2 the transfer from the measurement noise to the control signal is characterized by the two transfer functions H_N and H_V. Especially the magnitude for large values of Ω are of interest for further investigation. If the values of $|H_N(j\Omega)|_{\Omega\to\infty}$ and $|H_V(j\Omega)|_{\Omega\to\infty}$ are sufficiently small, the influence of the high-frequency disturbance is

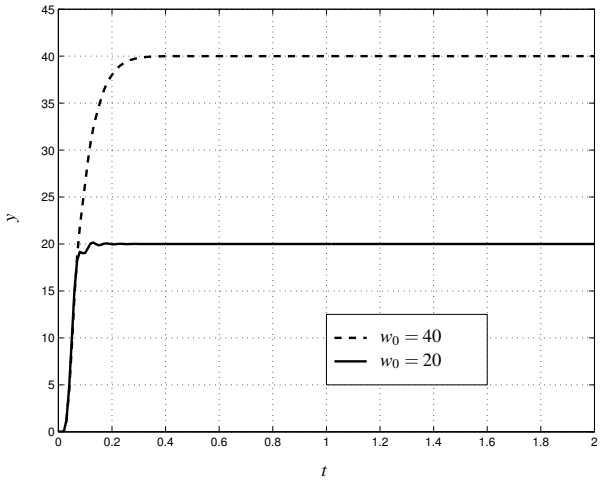

Fig. 9. System output with the adaptive Extension

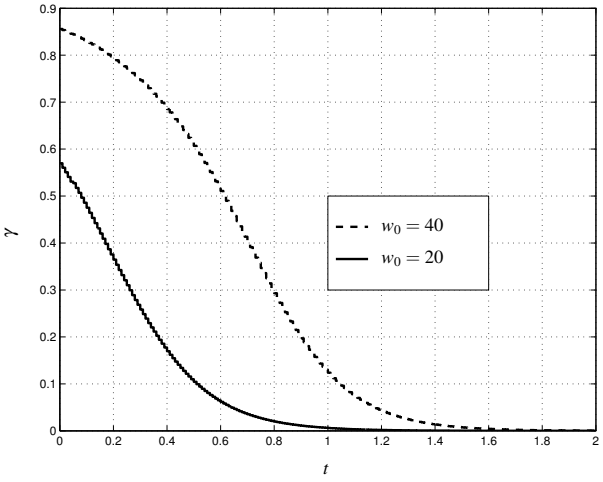

Fig. 10. Adaptive parameter γ for two operating points

small. Assuming lowpass behavior of the open loop without AW-Extension, the following relation results from (2):

$$|H_V|_{\Omega\to\infty} \approx \frac{-|\frac{G_{AW}}{R}|_{\Omega\to\infty}}{|1+\frac{G_{AW}}{R}|_{\Omega\to\infty}} \tag{19}$$

With a suitable choice of G_{AW}, the noise rejection properties can be influenced. The simulation example stated below confirms this assumption. The influence of measurement noise on the control loop with the coupled electric drives (12, 13) is investigated using different AW-Extensions (Deadbeat(Db)-observer [2], AW-Extension from 15 with $\gamma = 0.5$, AW-Extension from (7-10)). Fig. 11 shows E_{SQ} and in Fig 12 the magnitude $|H_V|$ can be seen. A larger sensitivity in the case of measurement noise for the Db-Observer can be seen in the curve of E_{SQ} and is confirmed by the values of $|H_V(j\Omega)|_{\Omega\to\infty}$.

V. Conclusion

This paper presents two design principles for Anti-Windup-Extensions of linear designed digital controllers.

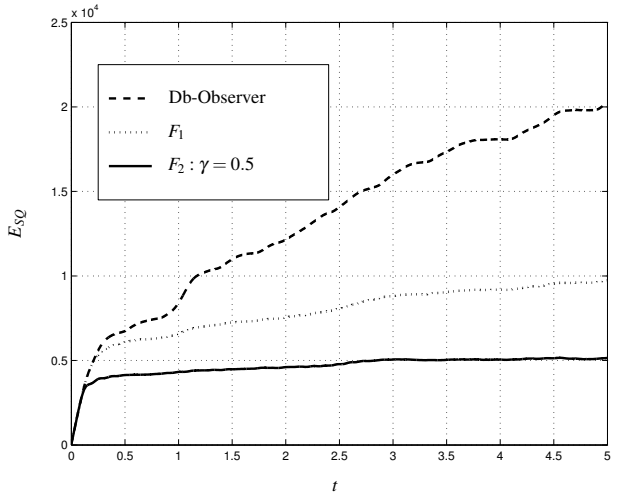

Fig. 11. E_{SQ} in the presence of noise for different AW-Schemes

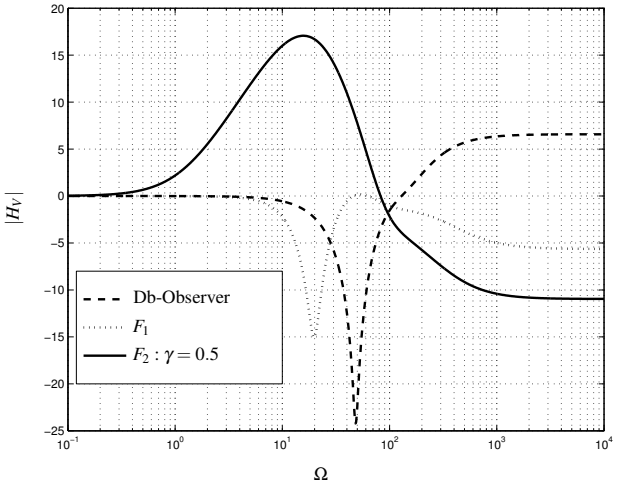

Fig. 12. Value characteristics of $|H_V|$ for different AW-Schemes

They are based on the use of a frequency characteristic response in the form of a bode plot. Therefore, they are graphically demonstrative and easy to use. The design reduces to a suitable choice of a phase shifting first order filter, which seems to be sufficient for most applications. The persistent design in the bode-diagram is believed to be new and leads to a simplification of the AW-Controller design.

A new adaptive structure for the AW-Extension is proposed, which is advantageous for the use in applications with a large operating range. The control performance with the use of the new structure is better than to adhere to fixed parameters.

In the last section it was shown that the chosen AW-Extension can have a significant influence on the noise rejection properties of the control loop. This influence can also be easily investigated by the use of frequency response characteristics.

REFERENCES

[1] K. J. Astroem ; B. Wittenmark. *Computer Controlled systems - Theory and Design*. Prentice-Hall, Inc., 1990.

[2] S. Rönnbäck ; K. S. Walgama ; J. Sternby. An Extension to the Generalized Anti-Windup Compensator. In *Proceedings of the 13th IMACS World Congress on Computation and Applied Mathematics*, volume 3, pages 1192–1196, Dublin; Ireland, 1991.

[3] S. Rönnbäck ; M. Sternad. A Frequency Domain Approach to Anti-Windup Compensator Design. Technical Report Report UPTEC 93024R, Department of Technology, Uppsala University, Sweden, 1993.

[4] S. Rönnbäck. Nonlinear Dynamic Windup Detection in Anti-Windup Compensators. In *Proceedings of CESA 96 Multiconference ; Symposium on Control, Optimization and Supervision*, pages 1014–1019, 1996.

[5] C. W. Chan ; K. Hui. Design of compensators for actuator saturation. *Proceedings of the Institution of Mechanical Engineers , Part 1: Journal of systems and control engineering*, 209:157–164, 1995.

[6] C. W. Chan ; K. Hui. Design of stable actuator saturation compensators in the frequency domain. *IEE Proceedings / Control Theory and Applications*, 145(3):345–351, May 1998.

[7] K. Hui ; C. W. Chan. On Noise Rejection Property of Actuator Saturation Compensators. In *Proceedings of the 2nd Asian Control Conference Vol. II*, pages 531–534, July 1997.

[8] J. L. Henrotte. Conditioning technique: Applications and practical considerations. In *Computing and Computers for Control Systems*, pages 25–27, J. C. Baltzer AG, Scientific, Scientific Publishing Co. and IMACS, 1989. P. Borne et. al. (editors).

[9] S. Lambeck. *Analyse und Entwurf von Anti-Windup-Erweiterungen für zeitdiskrete Regler im Frequenzbereich*. PhD thesis, Technical University Ilmenau, Germany, 2003.

[10] A. H. Glattfelder ; J. Tödtli ; W. Schaufelberger. Stability Properties and Effects of Measurement Disturbances on Antiwindup PI- and PID-Control. *European Journal of Control*, 6:435–448, 2000.